Epitaxial crystallization during 600 °C furnace annealing of amorphous Si layer deposited by low-pressure chemical-vapor-deposition and irradiated with 1-MeV Xe ions

Jyoji Nakata

Citation: Journal of Applied Physics **82**, 5446 (1997); doi: 10.1063/1.365571
View online: http://dx.doi.org/10.1063/1.365571
View Table of Contents: http://scitation.aip.org/content/aip/journal/jap/82/11?ver=pdfcov
Published by the AIP Publishing

Epitaxial crystallization during 600 °C furnace annealing of amorphous Si layer deposited by low-pressure chemical-vapor-deposition and irradiated with 1-MeV Xe ions

Jyoji Nakata[a)]
NTT Basic Research Laboratories, 3-1 Morinosato-Wakamiya, Atsugi-shi, Kanagawa-ken, 243-01, Japan

(Received 23 May 1997; accepted for publication 2 September 1997)

The amorphous Si layers deposited by low-pressure chemical vapor deposition on (100)-crystal-Si substrates and subjected to Xe-ion-beam irradiation are crystallized epitaxially in a layer-by-layer fashion to the surface during 600 °C furnace annealing. Layer-by-layer crystallization can be accomplished by irradiating the layers with a 1-MeV Xe-ion-beam for a $2\times10^{15}/cm^2$ dose at 310 °C prior to furnace annealing. In all cases during furnace annealing that amorphous Si layers are polycrystallized or are grown vertically in isolated epitaxial-columnar-structures and then grown laterally into the amorphous region surrounding each column, the ion-beam-induced epitaxial crystallization (IBIEC) method epitaxially crystallizes them in a layer-by-layer fashion. This is because O atoms that were at the initial interface and that prevented layer-by-layer crystallization or columnar-epitaxial-growth diffuse remarkably because of irradiation. This diffusion decreases the peak concentration and facilitates layer-by-layer crystallization. O atoms at the interface are also diffused by irradiation with 80-keV P, 100-keV As, and 150-keV As ions. This diffusion results in the columnar growth during 600–800 °C furnace annealing. Whether layer-by-layer growth or columnar growth occurs during the furnace annealing depends on the peak concentration of oxygen at the interface. Direct evidence is shown that O diffusion is enhanced by the amount of inelastic electronic scattering of incident ion beam under the same elastic nuclear scattering conditions. The rates of IBIEC and of epitaxial crystallization during furnace annealing after 1-MeV Xe-ion-beam irradiation for a $2\times10^{15}/cm^2$ dose are affected by the amount of oxygen in the amorphous layer. The rate of layer-by-layer IBIEC using a 1-MeV Xe-ion-beam is nearly twice as high for a sample heated in the deposition furnace after evacuation as it is for a sample heated before evacuation. This difference is due to the smaller amount of oxygen in the amorphous Si layer of the former sample.
 [S0021-8979(97)05223-7]

I. INTRODUCTION

Over the past two decades there have been a number of experimental and theoretical studies on ion-beam-induced epitaxial crystallization (IBIEC).[1–14] Of particular interest are the low-temperature characteristics of this method. Amorphous Si layers on the crystal-Si substrates are epitaxially crystallized in a layer-by-layer fashion by IBIEC at temperatures as low as 150 °C, far below the 600 °C temperature needed for ordinary solid-phase epitaxial-growth (SPEG) during furnace annealing. The rate of IBIEC has also been shown to be increased by the inelastic electronic scattering that occurs when the amorphous Si layer is exposed to a mega-electron-volt heavy-ion-beam.[12,14]

IBIEC can also be used in the formation of silicon-on-insulator (SOI) structures.[1] This is because IBIEC is a low-temperature nonequilibrium process that provides results quite different from those of the usual equilibrium thermal process. Specifically, IBIEC is useful for forming SOI structures over a wide area. The most important point in forming a SOI structure over a wide area is to prevent the polycrystallization of an amorphous Si layer on a SiO_2 film. Because IBIEC is a low-temperature process, the polycrystallization can be avoided by irradiation at temperatures below those at which polycrystallization occurs.

Another application of IBIEC is in the fabrication of wide-gap semiconductors like SiC, or diamond in which epitaxial layers of good quality and *n*-type conductivity have not yet been obtained. There is a possibility that ion implantation of *n*-type dopant atoms followed by IBIEC will make the diamond substrate *n*-type due to all the nonequilibrium processes that cannot be achieved by the usual equilibrium thermal process. Furthermore, Si-based alloys containing C, Ge, or Sn atoms at concentrations that exceed those predicted from the equilibrium stoichiometric ratios can be obtained by using the nonequilibrium IBIEC process.[15,16] The present article, however, focuses on the formation of SOI structures over a wide area, and orders to do this by IBIEC or by furnace annealing. We first need to clarify such properties as the vertical crystallization rates of amorphous Si layers deposited by chemical vapor deposition (CVD) or molecular-beam-epitaxy (MBE). The properties of the interface between the Si substrate and the deposited amorphous Si layer should also be clarified, such as a natural-oxide thickness or stoichiometric ratio of O and Si atoms in the oxide which strongly affects the vertical crystallization. It is desirable that these deposited amorphous Si layers on SiO_2 films crystallize laterally at low temperature without polycrystallization, since liability to vertical crystallization results in the enlargement of the crystallized Si area on a SiO_2 film.

[a)]Electronic mail: jyojin@aecl.ntt.co.jp

 0021-8979/97/82(11)/5446/14/$10.00

To epitaxially crystallize the deposited amorphous Si layers by furnace annealing, it is necessary to remove a natural oxide before deposition or to form an amorphous layer beyond the deposited interface by low-energy ion-beam-mixing.[17,18] To remove a natural oxide, annealing at more than 1100 °C for 2 min or at 850 °C for 30–60 min under atmospheric pressure is needed before deposition.[19,20] In mixing the interface, very high doses of Si ($1\times10^{16}/cm^2$ to $8\times10^{16}/cm^2$) and energies of 50–130 keV are needed to laterally crystallize the deposited amorphous Si layer on a SiO_2 film to a length of a few micrometers.[17] A clean interface has also been formed by using a relatively expensive procedure including sputter cleaning as well as annealing under an ultrahigh vacuum pressure.[21] Hung and co-workers succeeded in layer-by-layer epitaxial crystallization at 550 °C by using a conventional NH_4OH/H_2O_2 cleaning procedure in which HF/H_2O dipping was the final process.[22,23] They deposited amorphous Si layers at room temperature and under a pressure of about 2×10^{-7} Torr, and measured the areal densities of oxygen at the deposited interfaces. They correlated these densities with the crystallization appearance of the deposited amorphous Si layers. Their results and ours are compared in detail in Sec. IV A 7 and IV B 3.

This article reports on the properties of the interfaces between the amorphous Si layers grown by low-pressure CVD (LP-CVD) and the crystal-Si substrates those layers were grown on. It focuses on the decreased concentration of oxygen at interfaces by ion beam irradiation with various energies. The amorphous layer properties such as the vertical crystallization rates induced by IBIEC for samples processed in different ways are also reported in terms of O content in them.

It will be shown here that the amorphous Si layers grown by LP-CVD are epitaxially crystallized to the surface in a layer-by-layer fashion during 600 °C furnace annealing in a dry Ar ambient. This crystallization is made possible by irradiating the layers with a 1-MeV Xe-ion-beam (to a dose level of $2\times10^{15}/cm^2$) at 310 °C before the furnace annealing. This irradiation facilitates the diffusion of O atoms, and thus decreases the peak concentration of oxygen at the interface.

It will be also shown that O profiles at the deposited interfaces are spread out by irradiation with 80 keV P, or 100-keV As, or 150-keV As ions, and that this irradiation results in the growth of isolated epitaxial columns during furnace annealing at temperatures between 600 and 800 °C. It will also be clearly shown, under the same nuclear scattering conditions and under the same substrate temperature, that this irradiation enhances O diffusion by an amount that increases with the amount of inelastic electronic scattering.

Furthermore, it will be shown that the rate of layer-by-layer IBIEC induced by using a 1-MeV Xe-ion-beam is nearly twice as high for a sample heated in the deposition furnace after evacuation as it is for a sample heated before evacuation. This difference is explained in terms of the smaller amount of oxygen in the amorphous layer of the former sample.

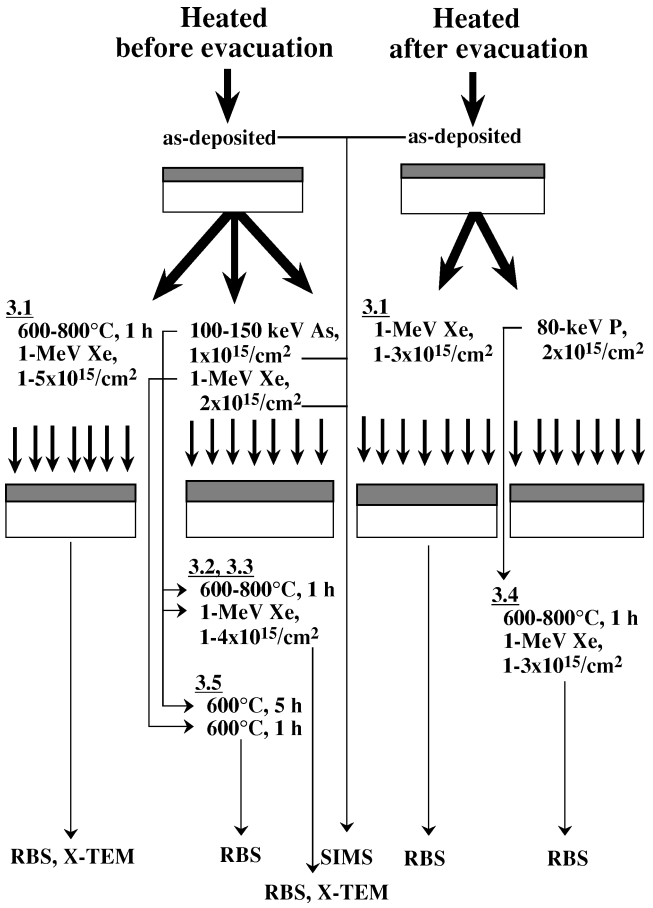

FIG. 1. Experimental procedure.

II. EXPERIMENTS

Experimental procedures, including both sample preparations and sample measurements, are shown schematically in Fig. 1. The underlined numbers (*3.1–3.5*) in Fig. 1 are those of Secs. III A–III E in which results are shown.

A. Sample preparation

The 4-in. *p*-type Si (100) wafers with a resistivity of 5–10 Ω cm were cleaned by using a H_2SO_4/H_2O_2 solution and were etched by using a diluted HF etchant in order to remove a natural oxide. They were then immediately put into the LP-CVD deposition furnace where amorphous Si layers 70–80-nm-thick were formed on them.

In the first set of experiments, the deposition furnace had been heated beforehand to 515 °C under a pressure of about 0.2 Torr. Then the furnace was vented with N_2 gas and was opened to load wafers into it. Wafers were then put into the furnace under atmospheric pressure and at temperatures from room temperature (RT) to 515 °C. The furnace was then evacuated and flowing Si_2H_6 gas was used to deposit amorphous Si layers onto the wafers.

In the second set of experiments, the wafers had been put into the furnace at RT under atmospheric pressure and then the furnace was evacuated. After it was heated to 515 °C, flowing Si_2H_6 gas was used to deposit the amorphous Si layers.

After deposition, in order to form amorphous Si layers of 100–140 nm thicknesses beyond the deposited interface, the interfaces of the samples in the first set of experiments were intermixed by irradiation with 100- to 150-keV As ions to a dose of $1\times10^{15}/\mathrm{cm}^2$, and the interfaces of the samples in the second set of experiments were intermixed by irradiation with 80-keV P ions to a dose of $2\times10^{15}/\mathrm{cm}^2$. A 200-keV conventional implanter was used and the beam current was 100–150 μA. The irradiation resulted in a wafer temperature rise of 150–200 °C (measured by thermo-labels attached to the surface of the wafer). The interfaces of the samples in the first set of experiments were also intermixed by 1-MeV Xe ions to a dose of $2\times10^{15}/\mathrm{cm}^2$ at 310 °C for a 0.6 μA/4 cm^2 dose rate, by using a 2.5-MeV Van-de-Graaff accelerator. Part of the 4-in. Si wafer was irradiated through a 2 $\times$2-cm mask. In contrast to the what happened when the kilo-electron-volt irradiation was used, amorphous Si layers were not formed entirely beyond the initial interface, when the mega-electron-volt irradiation was used, even though the energy density deposited at the interface as a result of the elastic nuclear-collision process was twice the energy density obtained when the kilo-electron-volt irradiation was used. This is due to the effective ion-beam-annealing effect caused by the large inelastic electronic scattering of the incident mega-electron-volt ion-beam.[24] The surface temperature of the wafer during the Xe-ion-beam irradiation used for intermixing and IBIEC was measured beforehand by an alumel–chromel thermocouple attached to the surface of the sample wafer by silver paste. During 1-MeV irradiation for a 0.6-μA/4 cm^2 dose rate it was 310 °C.

Two methods were used to crystallize these low-energy-intermixed and high-energy-intermixed amorphous Si layers: IBIEC using a 1-MeV Xe-ion-beam to $1-4\times10^{15}/\mathrm{cm}^2$ doses at 310 °C, and furnace annealing at temperatures between 600 and 800 °C for 1–5 h in a dry Ar ambient.

As-deposited wafers without mixing in both sets of experiments were also subjected to IBIEC using a 1-MeV Xe-ion-beam for $1-5\times10^{15}/\mathrm{cm}^2$ doses or to furnace annealing at 600–800 °C for 1 h.

B. Sample measurement

Samples were characterized by Rutherford backscattering spectroscopy (RBS) in the [100]-channeling direction. A well-collimated ($<0.03°$) 1.5-MeV He^+ ion beam 1 mm in diameter was directed into the sample, and backscattered He^+ ions or He atoms were detected by a silicon surface barrier detector (with a resolution of about 12 keV) that was set at a 110° angle to the probe-beam direction in order to improve the depth resolution. The He beam current was kept constant at a few nanoamperes and the integrated current was 2.6 μ C in all the channeling spectra shown in the next Sec. III. The energy resolution of the RBS system measured as the full width at half-maximum (FWHM) of the Si surface peak in the channeling spectrum was about 18 keV. The peak plateaus in the RBS spectra shown in Sec. III correspond to signals backscattered from amorphous Si layers. Energy width ΔE of each plateau is proportional to the thickness Δx of amorphous Si layer, and are expressed by the following equation:

$$\Delta E=[S]\Delta x,$$

where $[S]$ is the S factor (estimated to be 1100 eV/nm in the present experimental configuration). In all the channeling spectra in Sec. III, each channel has an energy width of 4 keV. Therefore, one channel corresponds to a depth range of about 3.6 nm in the amorphous Si layer and the Si substrate.

The crystallized layers were observed by cross-sectional transmission electron microscopy (X-TEM), and the O and H depth profiles in the amorphous Si layers were measured by high-resolution secondary-ion-mass-spectroscopy (SIMS). The background (B.G.) level of the O concentration was about $10^{18}/\mathrm{cm}^3$ and that of the hydrogen was about $10^{19}/\mathrm{cm}^3$. The resolution of the SIMS is estimated, from the FWHM of the O profiles at the amorphous–crystalline (a/c) interface in a sample just after deposition, to be about 4.5 nm (see Sec. IV A 3).

III. RESULTS

As schematically shown in Fig. 1, results in Secs. III B, C, and E are for the samples prepared in the first set of experiments and those in Sec. III D are for the sample prepared in the second set of experiments. In Sec. III A, a part of the results is for the samples in the first set of experiments and the rest is obtained from the samples in the second set of experiments.

A. As-deposited samples

Figure 2 shows the [100]-channeling spectra for as-deposited LP-CVD amorphous Si layers before and after furnace annealing (a), and before and after IBIEC (b). These samples were prepared in the first set of experiments. It is clear from Fig. 2(a) that amorphous layers keep amorphous phases or grow in polycrystal phases during 600–800 °C furnace annealing for 1 h. This is due to a natural oxide residing at the deposited interface for around one-monolayer thickness. As shown in Fig. 2(b), however, IBIEC with a 1-MeV Xe-ion-beam induces layer-by-layer epitaxial crystallization at 310 °C. It takes a dose of $2\times10^{15}/\mathrm{cm}^2$ for crystallization to proceed beyond the deposited interface. After getting beyond the interface, the epitaxially crystallized thickness is proportional to Xe dose and for a $5\times10^{15}/\mathrm{cm}^2$ dose, the crystallinity is, as far as the channeling spectrum is concerned, close to that of the bulk crystal. As is mentioned in Sec. IV A 2, the initial $2\times10^{15}/\mathrm{cm}^2$ dose is utilized to diffuse O atoms at the deposited interface, enabling layer-by-layer epitaxial crystallization by 1-MeV Xe-ion-beam irradiation and by furnace annealing at 600 °C (see Fig. 8 in Sec. III E).

Figure 3 shows the X-TEM image for the sample crystallized by 1-MeV Xe-ion-beam irradiation at a dose of 5 $\times10^{15}/\mathrm{cm}^2$, a dose at which, according to the channeling spectrum in Fig. 2(b), crystallization proceeded to near the surface. This X-TEM photograph clearly shows that the amorphous Si layer was epitaxially crystallized to the surface and that there were few defects in the crystallized region. There were, however, a considerable amount of defects below 350 nm from the surface, near the projected range (R_p) of 1-MeV Xe ions. They were formed during IBIEC in the nuclear collision process by 1-MeV Xe ions with crystal-Si

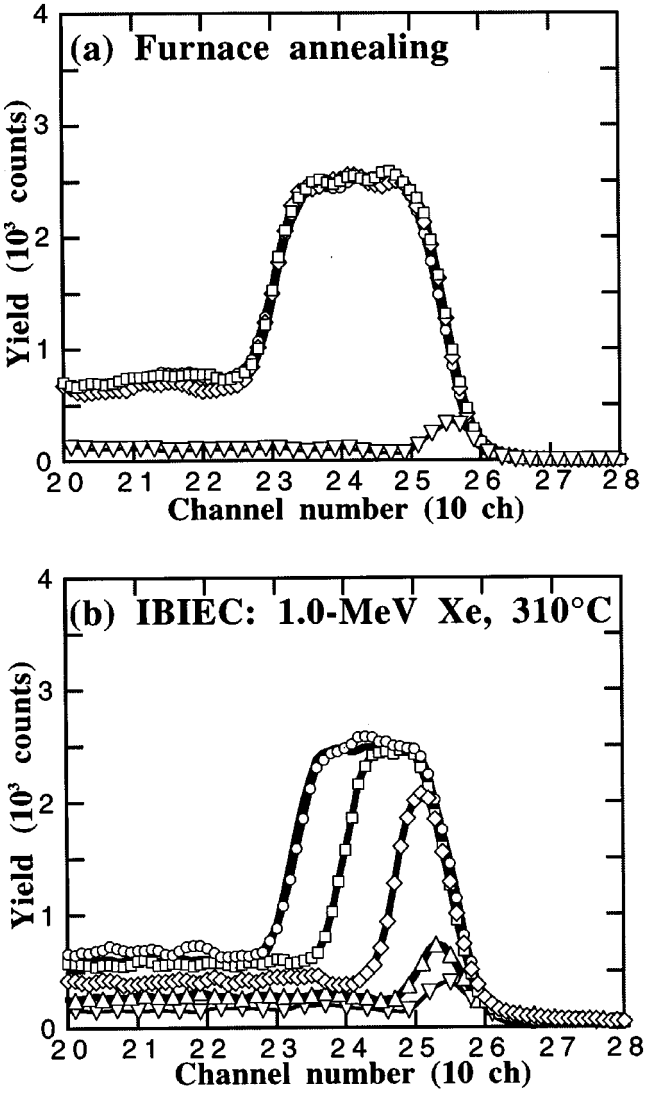

FIG. 2. [100]-channeling spectra for the as-deposited LP-CVD amorphous Si layers and for these layers after furnace annealing (a) or after IBIEC (b). Furnace annealing temperatures are 600 °C (○), 700 °C (□), and 800 °C (◇). The Xe doses are 2×10^{15}/cm^2 (○), 3×10^{15}/cm^2 (□), 4×10^{15}/cm^2 (◇), and 5×10^{15}/cm^2 (△). Solid line (superposed by blank-circle line) shows the spectrum of the as-deposited sample and ▽ shows that of the bulk-crystal Si.

substrates at 310 °C. Furthermore, a thin dark region around the deposited interface is seen, even though no defects can be seen in the channeling spectra in Fig. 2(b). This thin defect region observed by X-TEM may be due to vacancy-O complexes, which cannot be detected by the RBS-channeling measurements.

For the as-deposited sample prepared in the second set of experiments, the dose needed for the crystallization to proceed beyond the initial interfaces was the same as that for the sample prepared in the first set of experiments: 2×10^{15}/cm^2. The rate of IBIEC after 1-MeV Xe-ion-beam irradiation for a 2×10^{15}/cm^2 dose, however, was nearly twice that of the sample in the first set of experiments. The reason for the different rates of crystallization induced by IBIEC for the samples prepared in different ways is discussed in Sec. IV B in terms of the O content in those samples. Furthermore, these results are discussed in detail elsewhere,[25] along with the crystallization of the implantation-amorphized ultrahigh vacuum CVD epitaxial Si layer and the implantation-amorphized bulk-crystal Si substrate.

B. Sample intermixed by 100-keV As

Figure 4 shows the [100]-channeling spectra for LP-CVD amorphous Si layers intermixed by 100-keV As and then subjected to furnace annealing (a) or IBIEC (b). The 100-keV As mixing led to the formation of a 100-nm-thick amorphous Si layer (solid line) beyond the initial interface 80 nm from the surface (blank circle line). It is clear from Fig. 4(a) that although layer-by-layer epitaxial crystallization proceeded from the implantation-formed a/c interface to the initial interface at 600 °C but it stopped there, and the channeling yields decrease throughout the deposited amorphous layer as the annealing temperature increases from 600 to 800 °C. A similar decrease was also observed with increasing annealing time at the same temperature (not shown here). The decrease in channeling yields is evidence that, as is discussed later and shown in Fig. 9, at first the amorphous layer is vertically crystallized to the surface in isolated epitaxial-columnar-structures and subsequently the columnar crystal regions grow laterally into the surrounding amorphous regions.[22,23] An amorphous Si layer kept the amorphous phase or was converted into a polycrystal phase when the annealing temperature was 600 °C. The channeling yields do not change between the amorphous and polycrystal phases. This is discussed in Sec. IV A 1. Figure 4(b) shows that IBIEC, in contrast to the furnace annealing, induced layer-by-layer epitaxial crystallization at 310 °C. Furthermore, the Xe dose needed for crystallization to proceed beyond the deposited interface, and thus that needed to crystallize all the way to the surface, decreased because of pre-intermixing induced by 100-keV As irradiation. Thus IBIEC, which is a nonequilibrium process, is superior to the usual equilibrium thermal annealing in that it better prevents polycrystallization and that it better induces layer-by-layer epitaxial crystallization.

C. Sample intermixed by 150-keV As

Figure 5 shows the [100]-channeling spectra for LP-CVD amorphous Si layers intermixed by 150-keV As and then subjected to furnace annealing (a) or IBIEC (b). The 150-keV As mixing led to the formation of a 140-nm-thick amorphous Si layer far beyond the initial interface. It is clear from Fig. 5(a) that the columnar-crystal-structures grow throughout the deposited amorphous Si layer as the annealing temperature increases. Layer-by-layer epitaxial crystallization proceeded from the implantation-formed a/c interface to the initial interface but it stopped there for 600 °C annealing, as in the 100-keV As-mixing case. The extent of columnar-crystal-growth (that is, the extent of decrease in the channeling yields) at the same annealing temperature, however, is greater than that for the 100-keV As-mixing case shown in Fig. 4(a). Figure 5(b) shows that IBIEC, in contrast to the furnace annealing, caused the amorphous layer to epi-

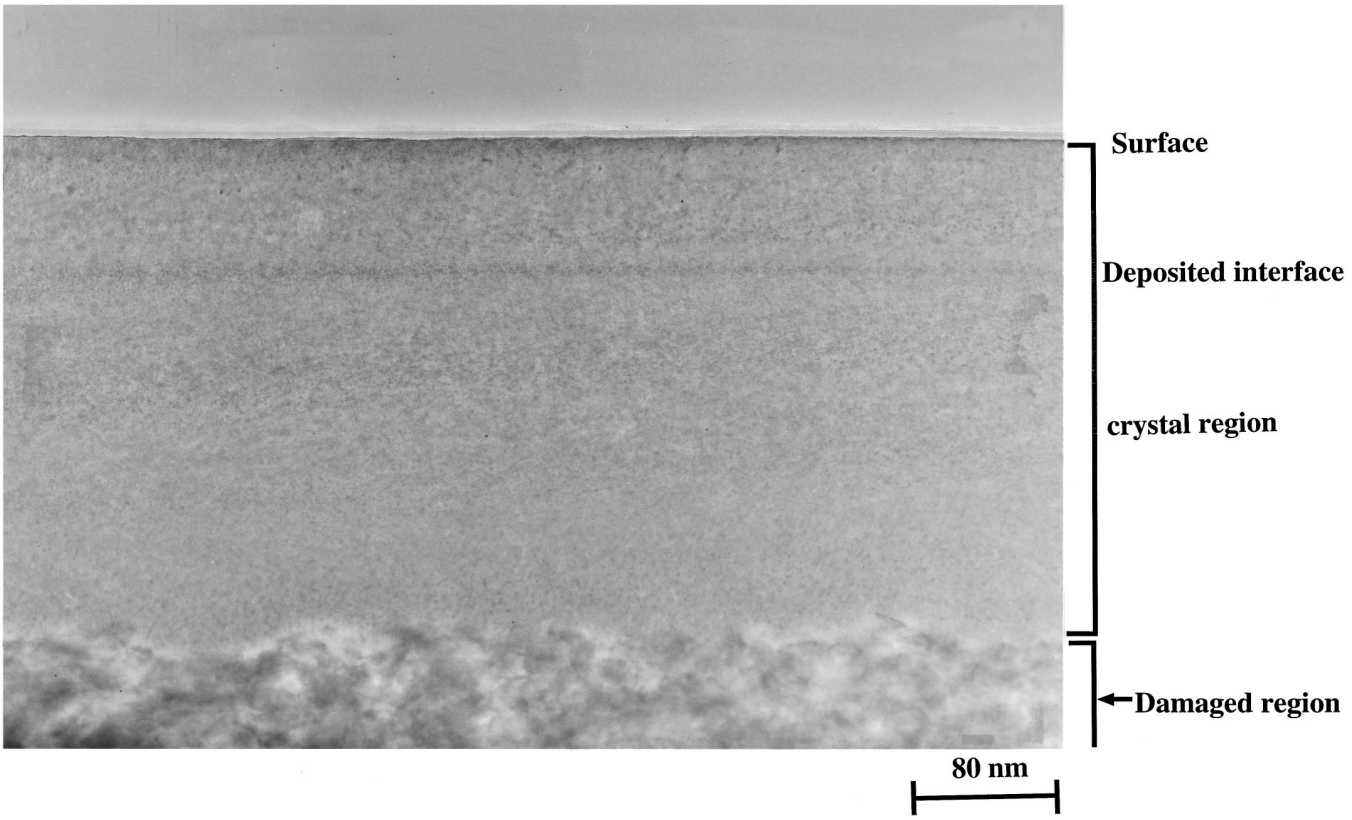

FIG. 3. X-TEM photograph showing the as-deposited sample crystallized to the surface by 1-MeV Xe-ion-beam irradiation at a dose of $5\times10^{15}/\mathrm{cm}^2$.

taxially crystallize in a layer-by-layer fashion. However, defects indicated by an arrow grew with Xe dose near the a/c interface formed by 150-keV As implantation. Furthermore, it is evident that the thickness of the layer-by-layer crystallized region tends to saturate with increasing Xe dose. This saturation is due to the accumulation of residual point defects after recombination of vacancies and recoiled-interstitials produced by the high dose of Xe ions. Accumulation retards vacancy migration and decreases the rate of IBIEC.[1]

Figure 6 shows an X-TEM image of the sample crystallized by IBIEC at a dose of 4×10^{15} cm^2. This dose induced layer-by-layer epitaxial crystallization nearly to the surface, but as mentioned above, a considerable number of defects were left near the implantation-formed a/c interface. A thin dark line at a depth of about 150 nm shows defects that were grown during IBIEC [indicated by an arrow in Fig. 5(b)] at doses greater than $4\times10^{15}/\mathrm{cm}^2$ and that were located just under the a/c interface formed by 150-keV As implantation. These secondary defects were formed in the partly damaged region in the crystal-Si substrate just under the implantation-amorphized layer, and have sometimes been observed when an implantation-amorphized Si layer formed at elevated substrate temperatures was crystallized by furnace annealing or IBIEC.

It seems from Fig. 5(b) that defects grown near the interface indicated by an arrow are completely within the implantation-amorphized layer. They actually are not, however, because the channeled He beam used for measuring the crystallized sample [that subjected to a Xe dose of $4\times10^{15}/\mathrm{cm}^2$ in Fig. 5(b)] loses less energy in the low-index channeling direction than does the one used for measuring the as-amorphized sample [solid line in Fig. 5(b)]. This is because a ''channeled'' He beam in the amorphous layer loses energy in the same manner as in the random direction of the crystal sample. Thus the position of the peak indicating the defect region shifts to a higher energy in the channeling spectrum.

Another type of heavily damaged region formed near the R_p of 1-MeV Xe ion can also be seen below about 350 nm in Fig. 6. It was grown, during 1-MeV Xe-ion-beam irradiation to a dose of $4\times10^{15}/\mathrm{cm}^2$ at 310 °C, in a nuclear collision process with the Si substrate. It is quite interesting that the initial interface at a depth of 80 nm can also be seen, although no yield increase is evident in the RBS channeling spectra in Fig. 5(b). This is the same result that was obtained after IBIEC for the as-deposited sample in Fig. 3. As mentioned in Sec. III A, it is possible that this thin defect region observed by X-TEM is due to vacancy-O complexes that are invisible in the RBS-channeling measurements.

D. Sample intermixed by 80-keV P

Figure 7 shows the [100]-channeling spectra for LP-CVD amorphous Si layers intermixed by 80-keV P and then subjected to furnace annealing (a) or IBIEC (b). These LP-CVD amorphous Si layers were formed in the second set of

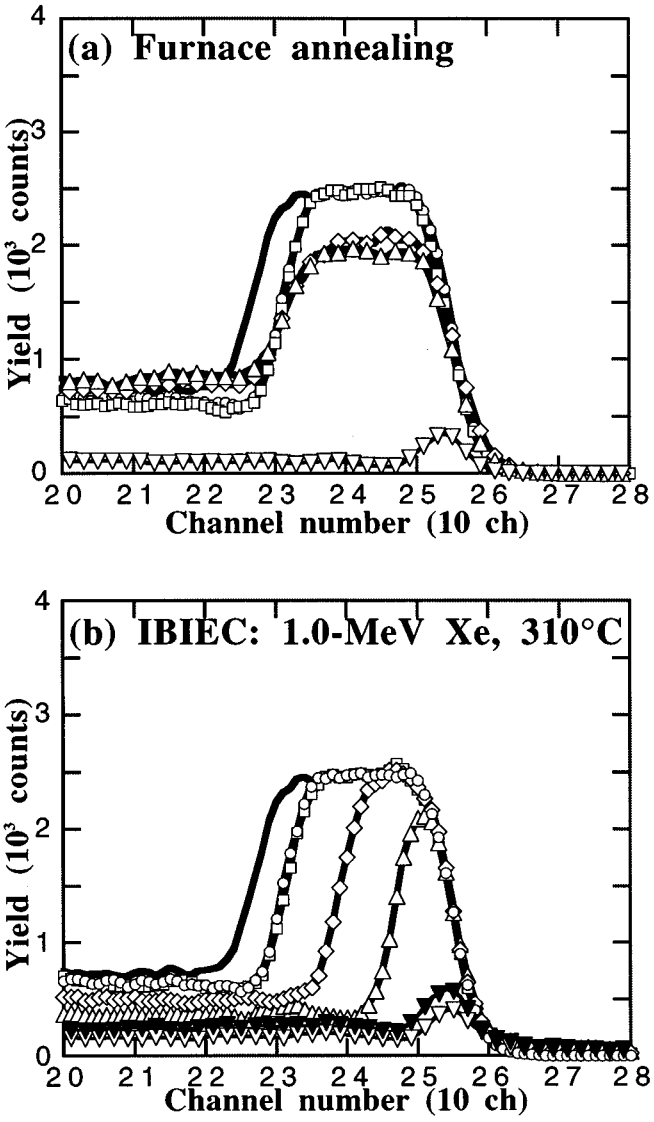

FIG. 4. [100]-channeling spectra for LP-CVD amorphous Si layers intermixed by 100-keV As and then subjected to furnace annealing (a) or IBIEC (b). Furnace annealing temperatures are 600 °C (□), 700 °C (◇), and 800 °C (△). Solid line and mark ○, respectively, show the spectra for the sample intermixed by 100-keV As and the as-deposited sample. Mark ▽ shows the spectrum for the bulk-crystal Si. The Xe doses are 1×10^{15}/cm^2 (□), 2×10^{15}/cm^2 (◇), 3×10^{15}/cm^2 (△), and 4×10^{15}/cm^2 (▼).

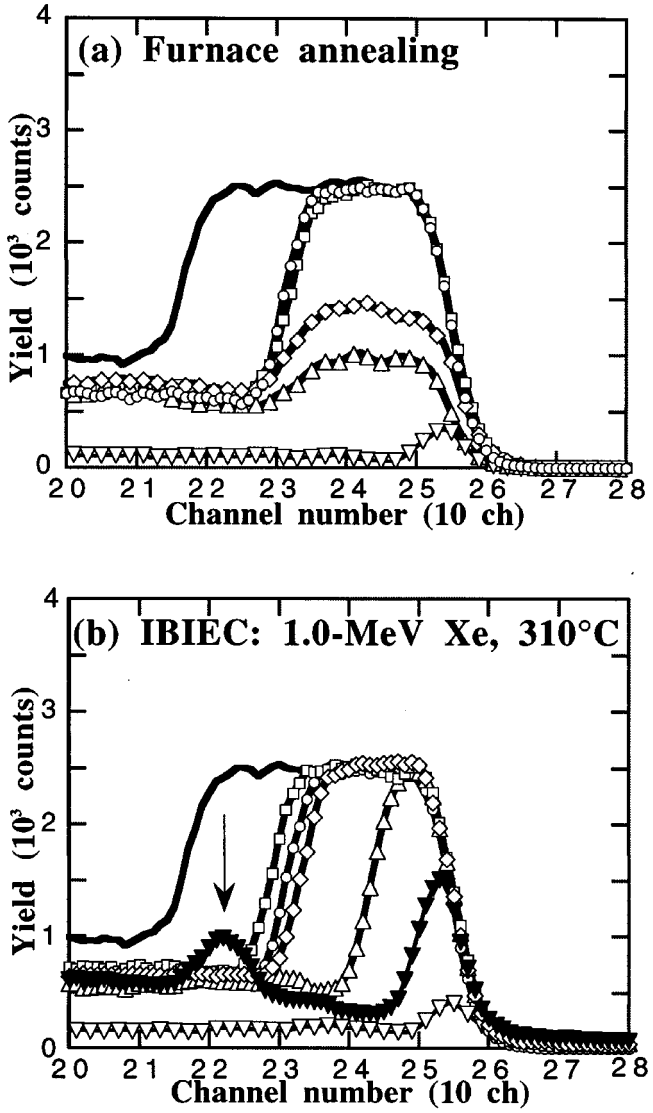

FIG. 5. [100]-channeling spectra for LP-CVD amorphous Si layers intermixed by 150-keV As and then subjected to furnace annealing (a) or IBIEC (b). Furnace annealing temperatures are 600 °C (□), 700 °C (◇), and 800 °C (△). Solid line and mark ○, respectively, show the spectra for the sample intermixed by 150-keV As and the as-deposited sample. Mark ▽ shows the spectrum for the bulk-crystal Si. The Xe doses are 1×10^{15}/cm^2 (□), 2×10^{15}/cm^2 (◇), 3×10^{15}/cm^2 (△), and 4×10^{15}/cm^2 (▼).

experiments. As shown in Fig. 7(a), the 80-keV P mixing led to the formation of 100-nm-thick amorphous Si layer beyond the initial interface at a depth of 70 nm. It is clear from this figure that the columnar-crystal-structures grow throughout the deposited amorphous Si layer as the annealing temperature increases. Layer-by-layer epitaxial crystallization proceeded from the implantation-formed a/c interface to the initial interface. However, it stopped there for 600 °C annealing, the same as for the 100- and 150-keV As-mixing cases shown in Figs. 4(a) and 5(a). The extent of columnar-crystal-growth at any given annealing temperature is the greatest among low-energy-mixing samples. In contrast to the furnace annealing, IBIEC induces epitaxial crystallization in a layer-by-layer fashion at the highest rate. The greater liability to crystallization by both IBIEC and furnace annealing for the sample prepared in the second set of experiments is mainly due to the lower concentration of oxygen in the deposited amorphous Si layers. This is discussed in Sec. IV B. Additionally, the liability to crystallization of the sample intermixed by P ions is partly due to the difference between the dopant effects of P ions and As ions. That is, the amorphous Si layer containing P atoms crystallizes more easily in both furnace annealing and in IBIEC than does an amorphous Si layer containing the same concentration of As atoms.[4,26]

E. Sample intermixed by 1-MeV Xe

In Secs. III B–III D, it became clear that the LP-CVD amorphous Si layers intermixed by low-energy ion-implantation can easily be vertically crystallized in isolated-columnar-structures during furnace annealing and that the

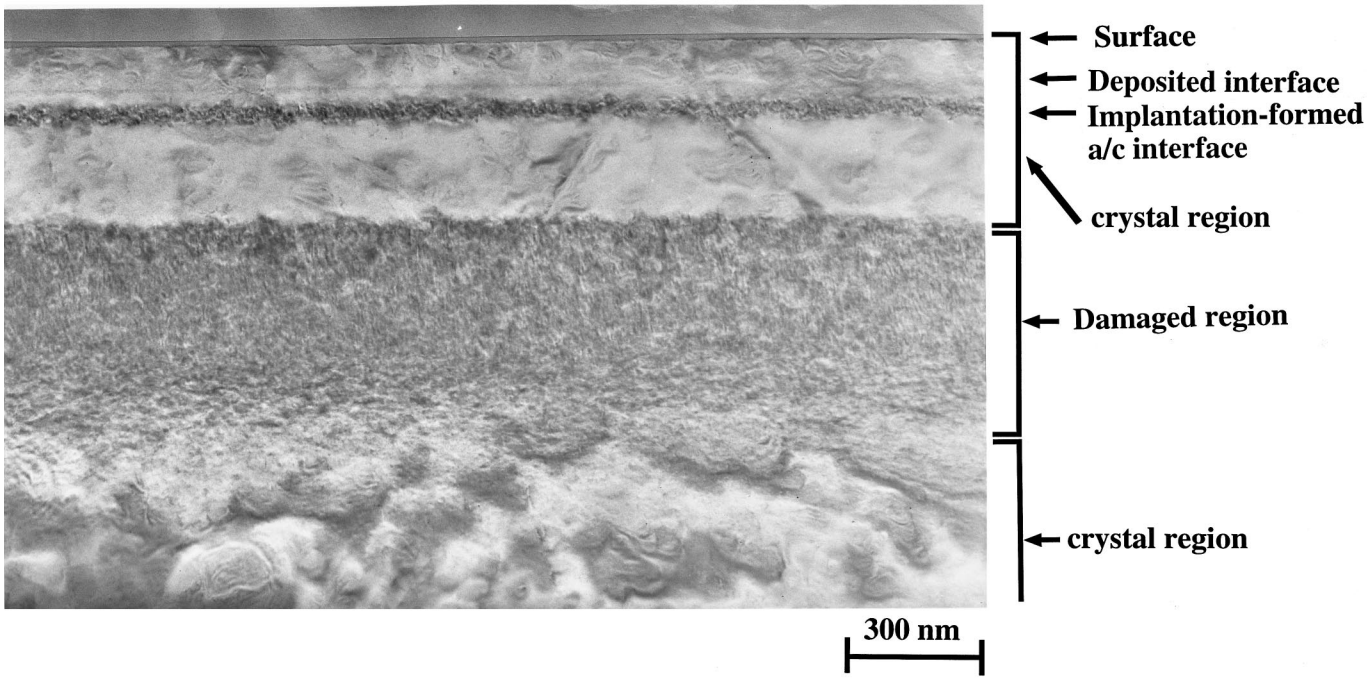

FIG. 6. X-TEM photograph showing the sample intermixed by 150-keV As and then crystallized by a 1-MeV Xe-ion-beam irradiation at a dose of $4\times10^{15}/\mathrm{cm}^2$.

liability to crystallization increases in the following order: 100-keV As, 150-keV As, and 80-keV P. If we use the same ion species for mixing, then the columnar-crystal-growth is more likely to occur as the mixing energy increases. The different appearances of columnar-crystal-growth in the P-mixing and As-mixing samples are thought to be mainly due to the different O contents in the amorphous Si layers processed in different ways and, as mentioned in Sec. III D, to be partly due to the differing dopant effects. The effect of oxygen on the crystallization rate is discussed in detail in Sec. IV B. Here I simply show the complete crystallization to the surface that can be induced by furnace annealing at 600 °C when the sample has first been subjected to 1-MeV Xe-ion-beam irradiation to a dose of $2\times10^{15}/\mathrm{cm}^2$ at 310 °C.

Figure 8 shows the [100]-channeling spectra for samples annealed at 600 °C for 1–5 h. Before the samples were annealed they were intermixed by 100–150 keV As implantation to a dose of $1\times10^{15}/\mathrm{cm}^2$ at 150–200 °C, and by 1-MeV Xe irradiation to a dose of $2\times10^{15}/\mathrm{cm}^2$ at 310 °C. As clearly seen from Fig. 8, the LP-CVD amorphous Si layer irradiated by a 1-MeV Xe-ion-beam was almost completely crystallized during annealing at 600 °C for 1 h. Samples intermixed by 100- to 150-keV As ions, however, were not crystallized or were columnarly crystallized during annealing at 600 °C for 5 h. The extent of columnar-crystal-growth increases with mixing energy from 120 to 150 keV, but for a 100-keV As-mixing sample, there is no columnar crystallization at all or there is a polycrystallization. An amorphous Si layer was epitaxially crystallized to the surface in a layer-by-layer fashion (not shown here) during furnace annealing at 600 °C for only 1 h when the sample had been irradiated by 1-MeV Xe ions at 310 °C prior to furnace annealing. As far as the channeling spectrum is concerned, the crystallinity is similar to that of the bulk crystal.

In consequence, it can be concluded that the liability of deposited amorphous Si layers to crystallization during furnace annealing can be enhanced by irradiating the layers with high-energy ions prior to furnace annealing.

IV. DISCUSSION

A. Interface properties

1. Interpretation of decreased channeling-yields

As pointed out in Sec. III B, the decreased channeling yields throughout the deposited amorphous Si layer can be explained by assuming that the isolated epitaxial-columnar-structures grow to the surface, and that this growth is followed by lateral crystallization into the surrounding amorphous region. The appearance of this crystallization is shown schematically in Fig. 9. It is thought that the growth of epitaxial columns first occurs independently at many isolated points or growth centers at the initial interface, where there are few or no O atoms and other impurities such as carbon.

Decreased channeling yields would also be observed if polycrystal Si grains were located uniformly throughout the layer and grew with increases in annealing time or temperature. For channeling-yield decrease to be observed in the RBS spectrum of such a structure, however, almost all the crystal-axes directions of the polycrystal grains must be oriented to those of the bulk-crystal Si substrate. An amorphous layer in which polycrystal Si grains with randomly oriented crystal-axes were distributed would, therefore, show the same channeling spectrum that an accurately amorphized

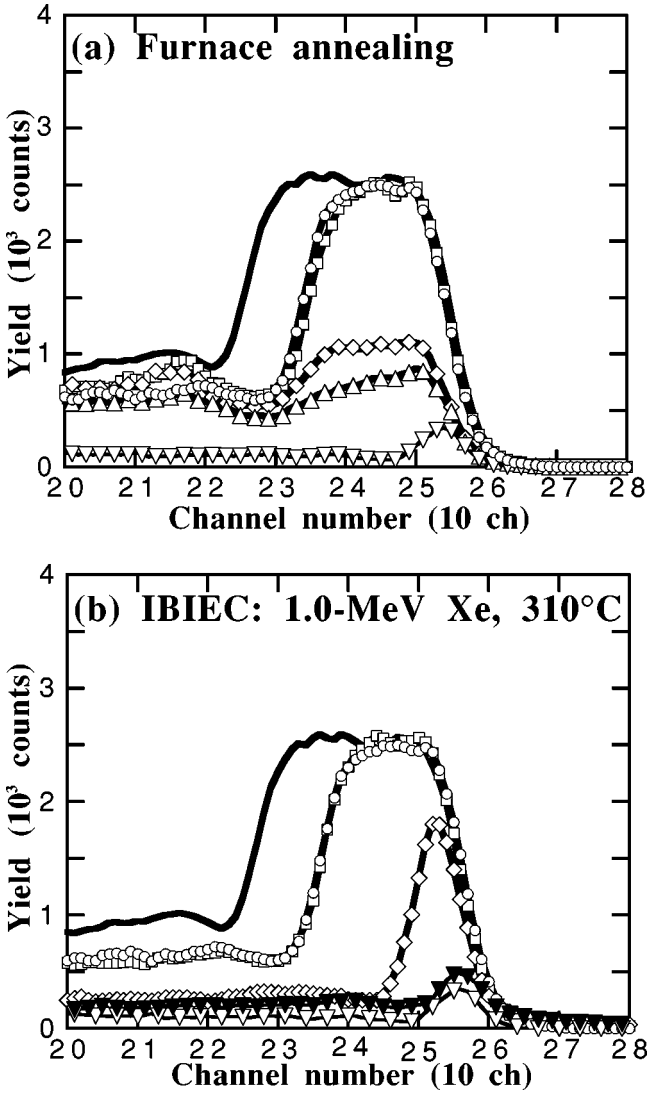

FIG. 7. [100]-channeling spectra for LP-CVD amorphous Si layers intermixed by 80-keV P and then subjected to furnace annealing (a) or IBIEC (b). Furnace annealing temperatures are 600 °C (□), 700 °C (◇), and 800 °C (△). Solid line and mark ○, respectively, show the spectra for the sample intermixed by 80-keV P and the as-deposited sample. Mark ▽ shows the spectrum for the bulk-crystal Si. The Xe doses are $1\times10^{15}/cm^2$ (□), $2\times10^{15}/cm^2$ (◇), and $3\times10^{15}/cm^2$ (▼).

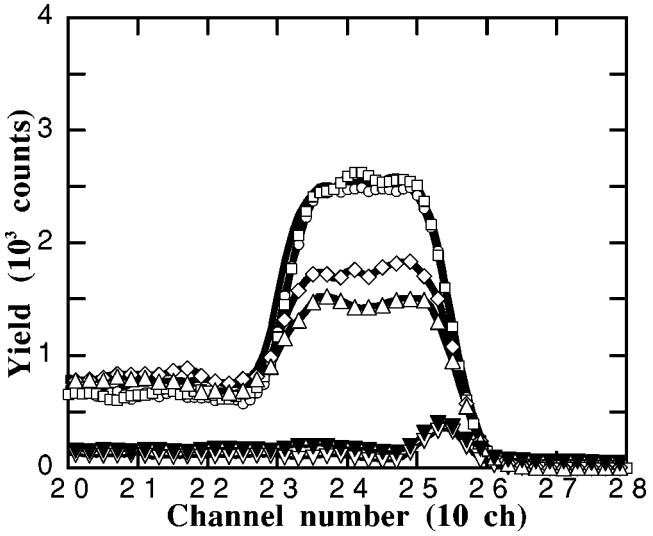

FIG. 8. [100]-channeling spectra for LP-CVD amorphous Si layers intermixed by 100- to 150-keV As ions or by 1-MeV Xe ions and then annealed at 600 °C for 1–5 h. The spectra are shown for the samples annealed at 600 °C for 5 h after as-deposition (○) and after 100-keV (□), 120-keV (◇), and 150-keV (△) As irradiation. The spectrum is shown for the sample annealed at 600 °C for only 1 h after 1-MeV (▼) Xe irradiation. Solid line shows the spectrum of the as-deposited amorphous Si layer before annealing and ▽ shows the spectrum of the bulk-crystal Si.

layer would. We thus cannot distinguish an amorphous-Si layer from a polycrystal-Si layer only from the RBS-channeling spectra in Fig. 2(a).

2. Oxygen diffusion at the interface by kilo- and mega-electron-volt ion beam irradiations

In Sec. III, the liability to layer-by-layer epitaxial crystallization during IBIEC and the liability to columnar-crystal-growth during furnace annealing were shown to be enhanced when the interface had been mixed by irradiating it with high-energy ions. This suggests that the high-energy irradiation decreases peak O concentration at the interface. O depth profiles of samples intermixed by various ions with various energies were therefore measured by high-resolution SIMS.

Figure 10(a) shows the depth profiles of oxygen at the initial interface before and after 100- and 150-keV As mixing. Arsenic doses for both mixing energies were $1\times10^{15}/cm^2$ and the temperatures measured during mixing were between 150 and 200 °C when the beam current was between 100 and 150 μA. These samples were prepared in the first set of experiments. The O profiles of the irradiated samples were almost the same as that of the as-deposited sample. They are only slightly broadened. Nevertheless, as shown in Figs. 4(a) and 5(a), columnar-epitaxial-growth occurred in the samples subjected to furnace annealing. To determine the O profiles precisely, however, it is necessary that the measured O profiles be deconvoluted with the finite depth resolution of the present SIMS apparatus. This is discussed in the following Sec. 3.

Figure 10(b) shows the O profiles of the same sample before and after intermixing by irradiation with a 1-MeV Xe-ion-beam to a dose of $2\times10^{15}/cm^2$ at 310 °C. O atoms diffused markedly. As mentioned in Sec. III E, a dose of $2\times10^{15}/cm^2$ before annealing was enough to result in layer-by-layer epitaxial crystallization during furnace annealing at 600 °C. And as shown in Fig. 2(b), this is also the minimum dose at which IBIEC proceeds beyond the CVD interface. It can be inferred from Fig. 10(b) that the threshold O concentration required for IBIEC to proceed beyond the interface or for layer-by-layer epitaxial crystallization to occur during furnace annealing is about $8\times10^{20}/cm^3$. Deposited amorphous Si layers containing less oxygen than this at the interface are expected to be crystallized epitaxially in a layer-by-layer fashion during furnace annealing.

3. Deconvolution of oxygen profiles

The areal densities of oxygen, that is, the integrated concentrations per unit volume to the depth direction plotted in Figs. 10(a) and 10(b), are all about $1\times10^{15}/cm^2$ for the first

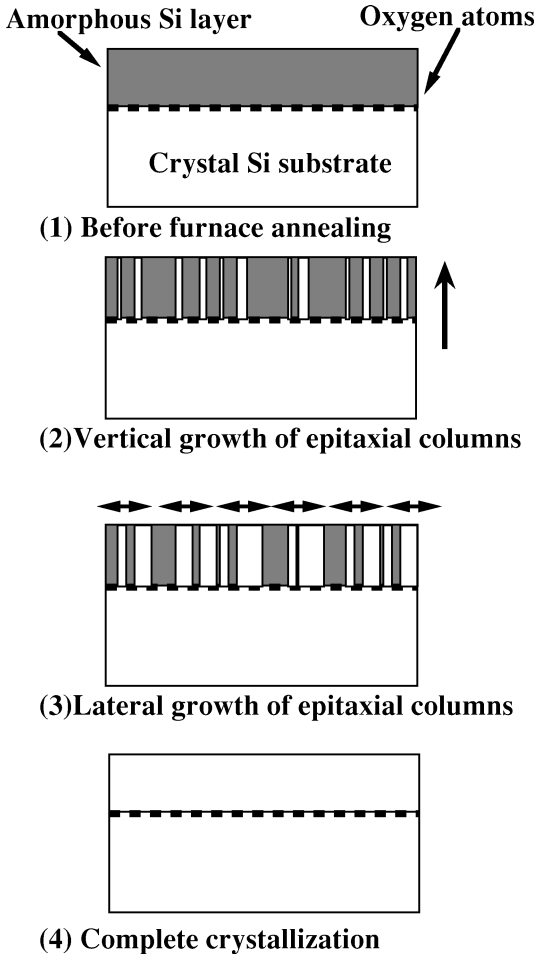

FIG. 9. Vertical growth of isolated-epitaxial-columns followed by lateral growth of each column into the surrounding amorphous region.

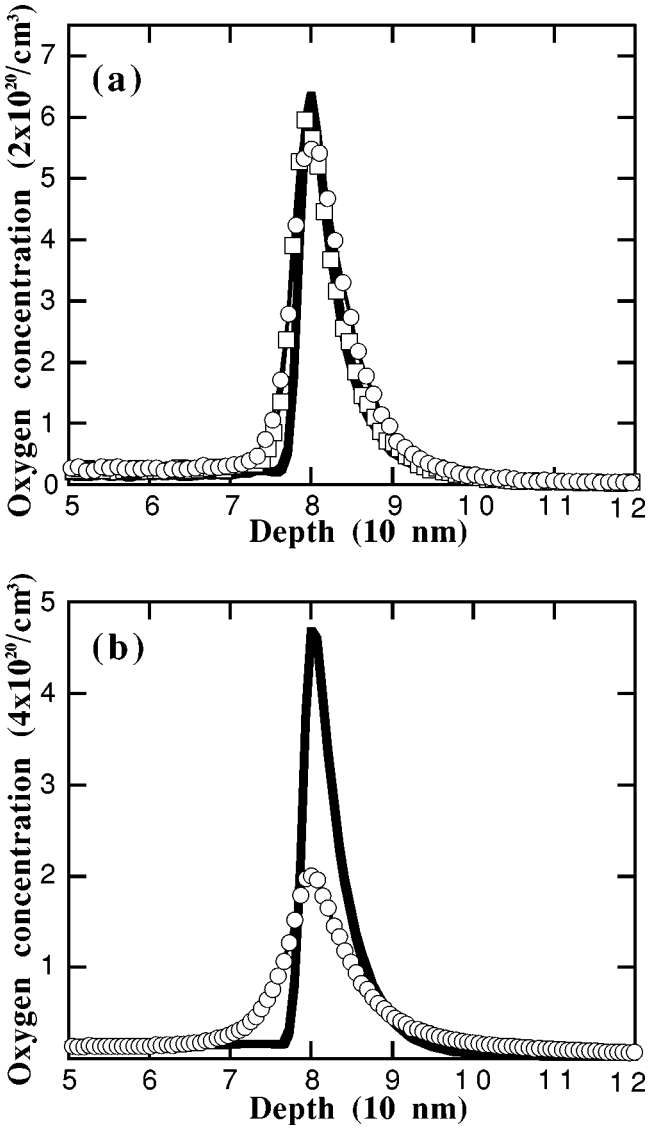

FIG. 10. O profiles at the deposited interface for (a) a sample just after deposition (solid line) and for samples intermixed by 100-keV (□) and 150-keV (○) As ions, and for (b) a sample just after deposition (solid line) and for one intermixed by 1-MeV Xe ions (○).

set of experiments. As mentioned in Sec. IV B, the areal densities for the second set of experiments are also about $1\times10^{15}/\mathrm{cm}^2$. If the oxide layer at the interface is silicon-dioxide and the density of silicon-dioxide is 2.20 $\mathrm{g/cm}^3$, the areal density of $1\times10^{15}/\mathrm{cm}^2$ corresponds to a dioxide-layer thickness of only 0.23 nm. A natural oxide, on the other hand, is thought to be no more than 1.5-nm-thick.[27] Here the deconvoluted-width of O profiles is estimated assuming two thicknesses for the dioxide layer in the as-deposited sample: 0.23 and 1.5 nm. From Figs. 10(a) and 10(b), the measured FWHM can be estimated to be 4.5 nm for the as-deposited sample, 6.0 nm for the 100-keV-As-irradiated sample, 7.6 nm for the 150-keV-As-irradiated sample, and 9.0 nm for the 1-MeV-Xe-irradiated sample. If we assume the depth resolution of SIMS to be Δx nm and the ''real thickness'' of oxide at the interface for the as-deposited sample to be either 0.23 or 1.5 nm, then we can estimate different depth resolutions from the following two equations:

$$0.23^2+\Delta x^2=4.5^2,$$

$$1.5^2+\Delta x^2=4.5^2.$$

Thus two only slightly different values of depth resolution are obtained: 4.5 and 4.2 nm. We can estimate the deconvoluted FWHM Δy of the oxide-widths in two ways for the intermixed samples from the directly measured FWHM values in Figs. 10(a) and 10(b) and from the two depth resolutions Δx obtained above:

$$4.5^2+\Delta y^2=6.0^2,7.6^2,9.0^2,$$

$$4.2^2+\Delta y^2=6.0^2,7.6^2,9.0^2.$$

Finally, we can write down real thicknesses Δy in two ways: 0.23 nm for the as-deposited sample, 4.0 nm for the 100-keV-As-irradiated sample, 6.1 nm for the 150-keV-As-irradiated sample, and 7.8 nm for the 1-MeV-Xe-irradiated sample and as 1.5 nm for the as-deposited sample, 4.2 nm for the 100-keV-As-irradiated sample, 6.3 nm for the 150-keV-As-irradiated sample, and 7.9 nm for the 1-MeV-Xe-irradiated sample. The FWHM values deconvoluted by different depth resolutions are about the same in each intermixed sample, except for the as-deposited sample, the oxide thickness of which is arbitrary assumed.

In both cases for different depth resolutions, Δy increases moderately with increasing intermixing energy in the range from kilo-electron-volts to mega-electron-volts. It should be noted that this moderately increasing appearance is quite different from that of the FWHM of the measured profiles in Figs. 10(a) and 10(b). Deconvoluting measured profiles makes it clear that radiation-enhanced diffusion is pronounced even after 100-keV As irradiation and enhancement becomes more remarkable with increasing intermixing energy. O diffusion, thus, seems to be enhanced by the amount of inelastic electronic scattering of the mixing-ion-beam. To separate the effect of elastic nuclear collision from that of inelastic electronic collision, however, the amount of energy deposited in the elastic nuclear scattering process must first be clarified.

4. Calculation of energy deposition

The density distributions of total number of vacancies (proportional to the energy loss in the elastic nuclear collision process) calculated by code TRIM90 for various doses of various ions with various energies are shown in Fig. 11(a). Figures 11(b) and 11(c) also show the distributions of the energy density deposited in inelastic electronic scattering process such as ionization or excitation under the same irradiation conditions as for Fig. 11(a). These are calculated for full cascade calculation, assuming the displacement energy of Si to be 13 eV and binding energy to be 2 eV. The vertical line at 80-nm depth represents the position of the initial interface. It is to be noted that the density of vacancies markedly exceeds the atomic density of the crystal-Si substrate ($5\times10^{22}/\mathrm{cm}^3$). This is because the *in situ* beam-annealing effect during irradiation is not taken into account in TRIM calculation. In reality, effective annealing occurs during mega-electron-volt ion-beam irradiation.[24] Thus, as shown in Fig. 2(b), the Si substrate near the deposited amorphous layer keeps its crystal phase even after irradiation with a 1-MeV Xe-ion-beam to a dose of $5\times10^{15}/\mathrm{cm}^2$ at 310 °C.

Figures 11(b) and 11(c) clearly show that the amount of inelastic electronic scattering in the amorphous region increases in the following order: 100-keV As for a $1\times10^{15}/\mathrm{cm}^2$ dose, 150-keV As for a $1\times10^{15}/\mathrm{cm}^2$ dose, 80-keV P for a $2\times10^{15}/\mathrm{cm}^2$ dose, and 1-MeV Xe for a $2\times10^{15}/\mathrm{cm}^2$ dose. This order is identical to that of liability to columnar-crystal-growth during furnace annealing or to layer-by-layer epitaxial growth during IBIEC, as shown in Sec. III. Thus, liability to crystallization is thought to be closely related to the amount of inelastic electronic scattering of the incident ion beam. On the other hand, as seen from Fig. 11(a), the densities of the total number of vacancies created at the interface are nearly the same for irradiations with 80-keV P for a $2\times10^{15}/\mathrm{cm}^2$ dose, and with 100- and 150-keV As for $1\times10^{15}/\mathrm{cm}^2$ doses. However, that formed by irradiation with 1-MeV Xe ions at a $2\times10^{15}/\mathrm{cm}^2$ dose is about twice as high as that formed by kilo-electron-volt ions. Furthermore, the 310 °C substrate temperature during 1-MeV Xe-ion-beam irradiation is higher than the 150–200 °C substrate temperatures reached during kilo-electron-volt-induced intermixing. Thus, there remains a possibility that the greater extent of O diffusion caused by 1-MeV Xe-ion-

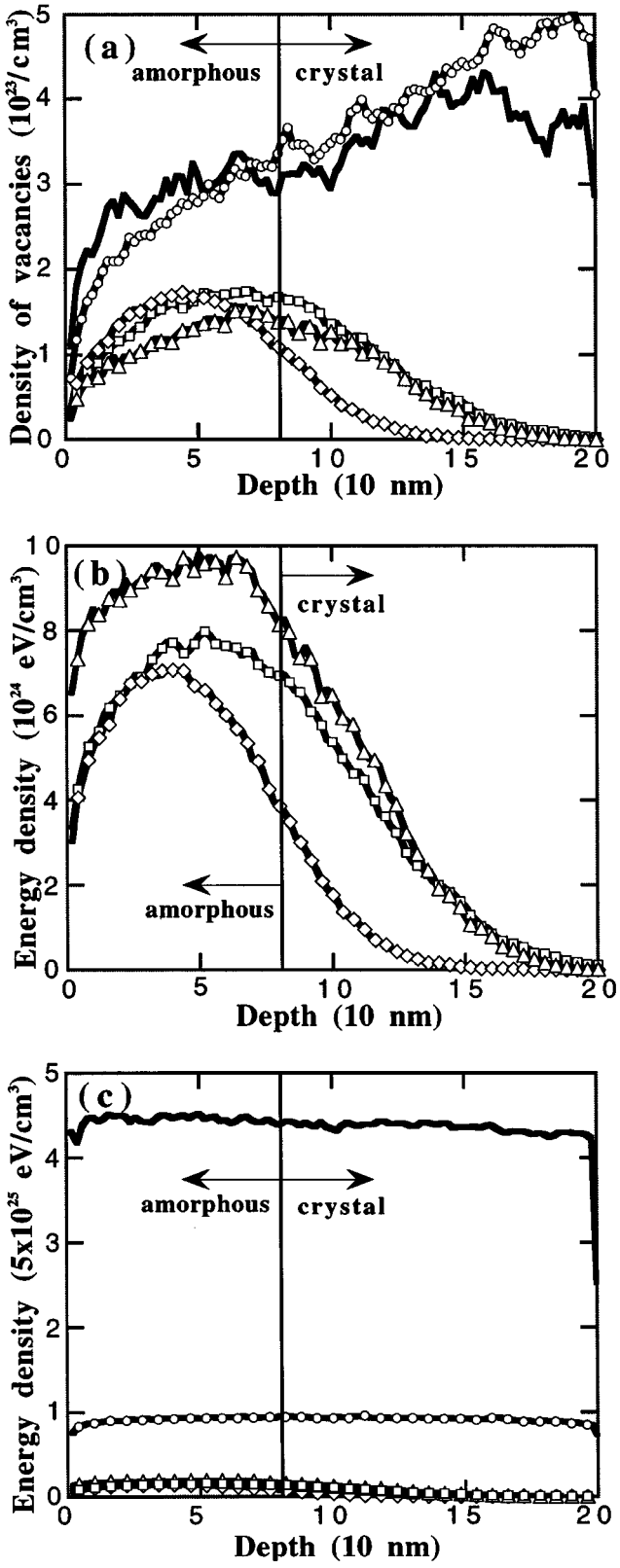

FIG. 11. (a) The density distributions of vacancies produced by various doses of various ions at various energies. Deposited-energy-density distributions due to inelastic electronic scattering of (b) kilo-electron-volt ions and (c) mega-electron-volt ions. Solid line: 5-MeV Xe for a $5\times10^{15}/\mathrm{cm}^2$ dose, ○: 1-MeV Xe for a $2\times10^{15}/\mathrm{cm}^2$ dose, □: 150-keV As for a $1\times10^{15}/\mathrm{cm}^2$ dose, ◇: 100-keV As for a $1\times10^{15}/\mathrm{cm}^2$ dose, △: 80-keV P for a $2\times10^{15}/\mathrm{cm}^2$ dose.

beam irradiation is due to two-times greater nuclear scattering and to a higher temperature during irradiation. Therefore, it cannot be concluded now that the greater extent of O diffusion shown in Fig. 10(b) is due to the inelastic electronic scattering effect. The enhancement of layer-by-layer epitaxial crystallization by enhanced vacancy diffusion due to inelastic electronic scattering, however, has been observed frequently and has been confirmed in the case of mega-electron-volt heavy-ion beam irradiation.[12,14]

5. Evidence for enhanced oxygen diffusion by inelastic electronic scattering

As mentioned in Sec. IV A 4, it is necessary to clarify the role of inelastic electronic scattering in the diffusion of oxygen under the same nuclear scattering conditions. An additional experiment was thus undertaken in order to examine the effect of varying the incident energy from 1 to 5 MeV under conditions in which the amount of nuclear energy deposited at the interface is the same and the substrate temperature is the same. The LP-CVD amorphous Si layers used for this experiment were prepared in the same way that those used in the first set of experiments were prepared.

Figure 12(a) shows [100]-channeling spectra for samples irradiated by 1-MeV Xe^{+} ions for a $2\times10^{15}/cm^2$ dose with a 0.75-μA/4 cm^2 dose rate at 310 °C and by 5-MeV Xe^{++} ions for a $5\times10^{15}/cm^2$ dose with a 0.3-μA/4 cm^2 dose rate (this dose rate corresponds to a 0.15-μA/4 cm^2 particle current) at 310 °C. The two doses were selected so that the same amount of nuclear energy would be deposited at the interface [see Fig. 11(a)]. Furthermore, the dose rates were also selected to produce the same beam power density, resulting in the same temperature rise: about 10 °C above the equilibrium 300 °C wafer temperature without irradiation. It is evident that even when the same amount of nuclear energy is deposited at the interface under the same 310 °C substrate temperature, 5-MeV Xe irradiation crystallizes the amorphous layer to near the surface whereas 1-MeV Xe irradiation does not entirely crystallize it.

Figure 12(b) shows the O depth profiles, on a linear scale, for the as-deposited sample and for the samples after 1-MeV Xe-ion-beam irradiation for a $2\times10^{15}/cm^2$ dose at 310 °C and after 5-MeV Xe-ion-beam irradiation for a $5\times10^{15}/cm^2$ dose at 310 °C. As clearly seen from Fig. 12, the O profile broadens and the peak concentration decreases more for 5-MeV irradiation than for 1-MeV irradiation. Figure 12(c) shows the same O depth profiles on a log-scale. Here it is also clear that oxygen diffused to a deeper region (100–200 nm) for 5-MeV irradiation than for 1-MeV irradiation. Furthermore, oxygen diffused to the surface and piled-up there for the 5-MeV-irradiated sample. Thus, it can be concluded that the O diffusion is enhanced by the inelastic electronic scattering of the incident ion beam.

In consequence, concrete evidence is clearly given that the diffusion of oxygen as well as layer-by-layer epitaxial crystallization induced by mega-electron-volt heavy-ion-beam irradiation are enhanced by the inelastic electronic scattering of the incident ion beam under the same elastic nuclear scattering conditions.

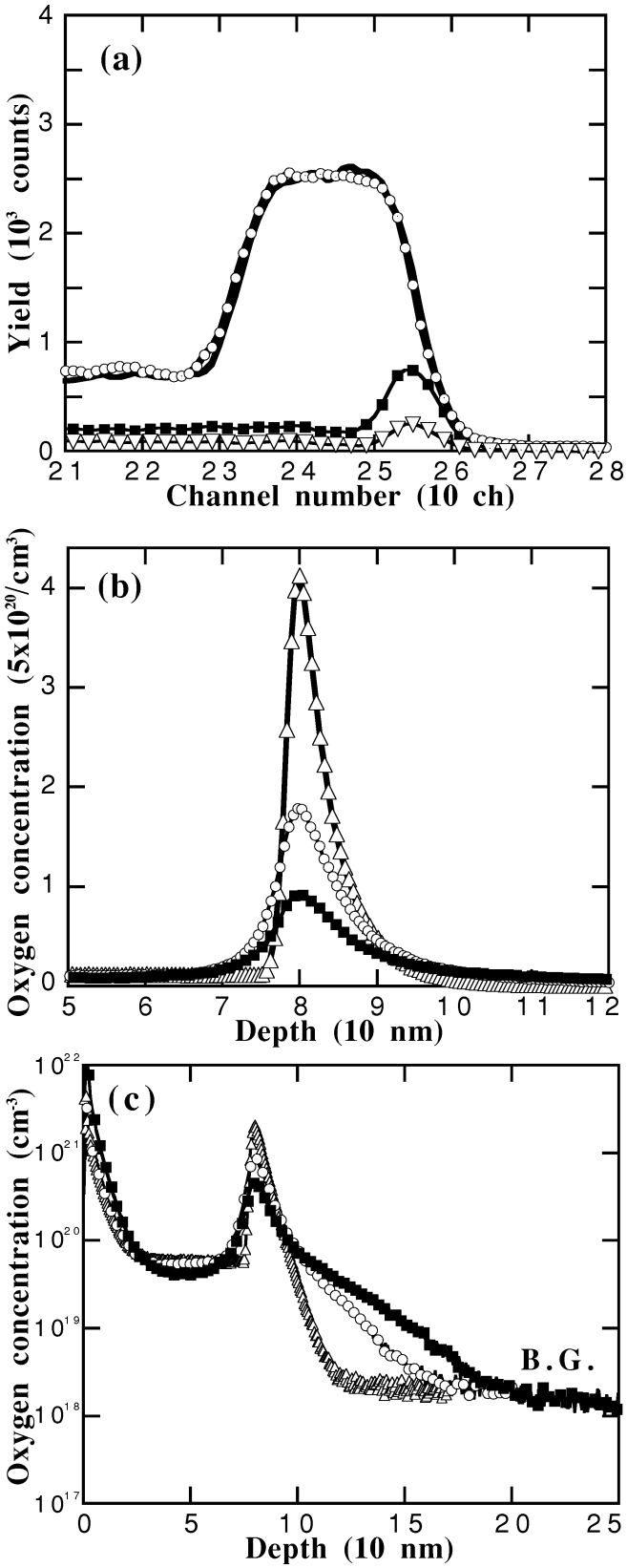

FIG. 12. (a) [100]-channeling spectra for LP-CVD amorphous Si layers irradiated by 1-MeV Xe ions for a $2\times10^{15}/cm^2$ dose (○) and by 5-MeV Xe ions for a $5\times10^{15}/cm^2$ dose (■) at the same substrate temperature (310 °C). Solid line and ▽, respectively, show the spectra for the as-deposited sample and the bulk-crystal Si. O profiles at the deposited interface measured by high-resolution SIMS and shown on (b) linear and (c) logarithmic scales: the sample just after deposition (△), the sample intermixed by 1-MeV Xe ions for a $2\times10^{15}/cm^2$ dose (○), and the sample intermixed by 5-MeV Xe ions for a $5\times10^{15}/cm^2$ dose (■). Substrate temperature=310 °C.

6. Mechanism of enhanced oxygen diffusion

Previous articles,[12,14] have reported that the rate of IBIEC was enhanced by the inelastic electronic scattering of an incident mega-electron-volt heavy-ion-beam. Possible mechanisms of this enhancement were discussed qualitatively on the basis of the review by Bourgoin and Corbett.[28] It was also reported[29] that the rate of transformation from hexagonal phase to tetragonal phase for WSi_2 samples, normalized by the nuclear energy deposition, increases with the inelastic electronic scattering of 0.5- to 5-MeV Xe-ion-beam irradiation. This suggests that Si atom migration to the W layers or defect migration is also enhanced by the inelastic electronic scattering of a mega-electron-volt heavy-ion-beam.

The role of inelastic electronic scattering caused by electron-beam and photon-beam irradiation in atomic migration phenomena at low-temperature has recently become a hot topic[30–35] in solid-state physics. Takahashi *et al.*[30] formed a GaAs quantum wire by using electron-beam-induced selective growth technology. A narrow quasiquantum GaAs wire can be formed by using *in situ* electron-beam irradiation and simultaneously supplying trimethyl-gallium and cracked AsH_3. Wada *et al.*[31–33] achieved low-temperature diffusion (doping), epitaxy, and oxidation by electron-beam irradiation of waters or metal layers on various substrate materials. Akazawa *et al.*[33] reported that photostimulated evaporation of amorphous SiO_2 and microcrystalline Si can be induced by synchrotron radiation in an ultrahigh vacuum and in a H_2 ambient. And Sato *et al.*[35] reported that by irradiating a 300-nm-thick amorphous silicon layer on a crystalline substrate with synchrotron-radiation x-rays at RT, they could induce homogeneous crystalline nucleation during the 600 °C postannealing process. They also reported that this irradiation greatly enhanced the recrystallization of amorphous Si at 500 °C. They attributed this irradiation-enhanced crystal growth process to vacancy-interstitial pair production caused by the Auger process.

Whereas almost all these reports have dealt with enhanced atom migration induced by electronic excitation or ionization associated with electron-beam or photon-beam irradiation, the present report emphasizes that in inelastic electronic scattering associated with mega-electron-volt heavy-ion-beam irradiation also enhances the migration of O atoms at the deposited interface. In the previous reports,[12,14,29] enhancement of vacancy migration or of Si atom migration was emphasized. Here O atom migration with the assist of inelastic electronic scattering of mega-electron-volt heavy-ion-beam irradiation is a main concern, but the discussion is essentially the same as for the vacancy migration or Si atom migration cases.[12,14,29] Detailed discussions can be found in Refs. 12 and 29.

7. Comparison with other authors' results

As explained in detail in Sec. II A, LP-CVD amorphous Si layers were prepared for the first and second set of experiments. The wafer cleaning procedures were the same for both sets of experiments, and a diluted HF dip was the final process before the wafers were put into the deposition furnace. Hung and co-workers[22,23] investigated the epitaxial crystallization of deposited amorphous Si layers and reported that the areal density of oxygen after a final HF dip was $0.5-1\times10^{14}/cm^2$, which is one order of magnitude lower than the density we measured. This lower O density enabled layer-by-layer epitaxial crystallization by furnace annealing. They also reported that the areal density of O atoms at the interface after HF immersion followed by rinsing with high-purity water was $2\times10^{14}/cm^2$. This slightly higher density caused the amorphous layer to grow first in isolated-epitaxial-columns and then laterally into the surrounding amorphous region (see Fig. 9). The difference between the interface O concentration we report and that which Hung and co-workers report can be attributed to the different substrate temperatures during deposition. Whereas our LP-CVD amorphous Si layers were deposited at 515 °C under a vacuum pressure of roughly 0.2-Torr, those of Hung and co-workers were prepared at RT under a high-vacuum pressure of 2×10^{-7} Torr. Somewhere in our process during temperature rising, the wafer surface was adsorbed by O atoms or by –O–H radicals for around $1\times10^{15}/cm^2$ density, as soon as H atoms that had terminated Si dangling-bonds after HF dipping dissociated and evaporated. In any case, such a high O density at the interface for as-deposited LP-CVD samples blocks even the columnar-crystal-growth, as shown in Fig. 2(a). After the peak O concentration was reduced by ion-beam-irradiation, however, columnar growth and even layer-by-layer growth occurred easily.

B. Amorphous layer properties

The rates of IBIEC and of layer-by-layer epitaxial crystallization by furnace annealing are strongly affected by the O content in the deposited amorphous Si layer. As mentioned in Sec. III A, regardless of whether samples were heated before evacuation or after evacuation, the same $2\times10^{15}/cm^2$ dose was needed if crystallization was to proceed beyond the CVD interface. But after irradiation to an ion dose of $2\times10^{15}/cm^2$ the layer-by-layer epitaxial crystallization proceeds and the rate of IBIEC in the sample heated after evacuation (the AFTER sample), is twice as high as that for the sample heated before evacuation (the BEFORE sample). The O concentrations in the BEFORE samples were expected to have been higher than those in the AFTER samples, so O profiles were measured by using high-resolution SIMS.

1. Oxygen profiles

Figure 13(a) shows the SIMS profiles of oxygen in the LP-CVD amorphous Si layers as well as in the amorphized bulk-crystal Si substrate. The peaks at the deposited interfaces are due to oxides formed while the temperature was rising to 515 °C, and plateaus in the amorphous layer are due to incorporation of O atoms during deposition. It is clear from Fig. 13 that the O concentration in the AFTER sample is about $2\times10^{19}/cm^3$, or about one third of that in the BEFORE sample. The small amount of oxygen in the AFTER sample leads to the two-times-higher rate of IBIEC. And notice that the concentration at the deposited a/c interface is about the same for both samples. This is why the same 2

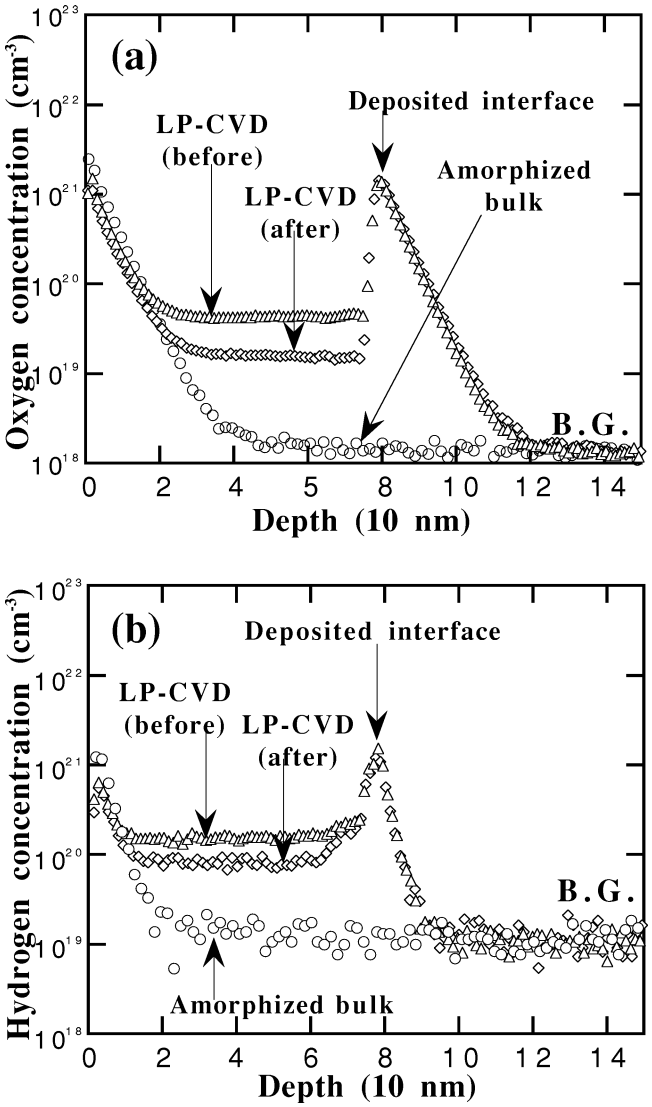

FIG. 13. (a) O and (b) H profiles in the LP-CVD amorphous Si layers and in the implantation-amorphized bulk-crystal Si substrate. The LP-CVD amorphous Si layers were formed in different ways. One (△) was deposited in a furnace that had been heated before evacuation, and the other (◇) was deposited in a furnace that had been heated after evacuation. Also shown are the profiles of hydrogen and oxygen for the implantation-amorphized bulk-crystal Si substrate (○).

$\times 10^{15}/\mathrm{cm}^2$ dose is needed for crystallization to proceed beyond the a/c interface. Furthermore, O concentrations in the two LP-CVD amorphous Si layers are much greater than that in the implantation-amorphized bulk-crystal Si substrate. Why the O concentration of the BEFORE sample is three times higher than that for the AFTER sample and why the O concentration at the deposited interface is nearly the same between two samples are not yet clear, but qualitative explanations can be given.

When the BEFORE sample was deposited, the furnace which had been kept at 515 °C was opened in order to put wafers into it. As soon as the furnace was opened, O and N molecules entered and some adsorbed to the wall of the furnace. While wafers were carried into the furnace, the wafer temperature rose from RT to 515 °C under atmospheric pressure. Thus, H atoms that had terminated Si dangling-bonds after the dipping in the HF solution dissociated and evaporated while the temperature was rising. O atoms that had entered the furnace when it was opened then immediately adsorbed to the surface of wafers and soon saturated at an areal density of $1\times 10^{15}/\mathrm{cm}^2$. O atoms that had been introduced into the furnace were also taken into the amorphous Si layers at a constant rate during deposition.

When the AFTER sample was deposited, wafers were first put into the furnace at RT. Therefore, the surfaces of Si wafers had been kept terminated by hydrogen atoms during the loading. Then the furnace was heated to 515 °C after it was evacuated to 10^{-3} Torr. Therefore the amount of oxygen in the furnace is expected, because of the evacuation before heating, to be much lower than it was when the BEFORE sample was prepared. When H atoms dissociated and evaporated during the time the temperature was rising, O atoms immediately adsorbed to the surface of the wafer. However, adsorption soon saturated to the same areal density, $1\times 10^{15}/\mathrm{cm}^2$. This value is probably determined by the temperature at which H atoms begin to dissociate and evaporate rather than by the O content in the furnace. Consequently, the amount of oxygen entering the amorphous Si layer during deposition is expected, because of the much smaller amount of oxygen introduced into the furnace, to be lower for the AFTER sample than for the BEFORE sample.

2. Hydrogen profiles

As shown in Fig. 13(b), H concentrations in the amorphous layers were around $10^{20}/\mathrm{cm}^3$ throughout the deposited amorphous Si layers for the two LP-CVD samples processed in different ways. There is only a negligible amount of hydrogen in the bulk sample. Some H atoms are also left at the deposited interface. If we rank the samples according to the rate of IBIEC starting with the highest, the order is: the implantation-amorphized bulk-crystal Si substrate, LP-CVD amorphous layers heated after evacuation, and LP-CVD amorphous layers heated before evacuation. The rates for the first and second samples, however, that is, for the bulk sample and the AFTER sample, are of about the same order. Thus to get the higher vertical-crystallization rate in both IBIEC and furnace annealing, there should be only a negligible amount of oxygen, which means a concentration below $2\times 10^{19}/\mathrm{cm}^3$. The incorporation of hydrogen into an amorphous Si layer has a great effect on the rate at which the layer crystallizes in the absence of oxygen. This is discussed in detail elsewhere.[25]

3. Comparison with other authors' results

Hung and co-workers reported[22,23] that the deposited amorphous Si layer formed under a pressure of about 2×10^{-7} Torr, containing oxygen at a concentration of $3\times 10^{19}/\mathrm{cm}^3$ and containing hydrogen at a concentration of $2\times 10^{20}/\mathrm{cm}^3$ shows nearly the same rate of layer-by-layer epitaxial crystallization during furnace annealing that the implantation-amorphized bulk-crystal Si substrate does. Here we obtained similar results in that the rate of IBIEC for the LP-CVD amorphous Si layer containing $2\times 10^{19}/\mathrm{cm}^3$ oxygen with a H content of around $10^{20}/\mathrm{cm}^3$ (AFTER sample in

Fig. 13) was nearly the same as that for the implantation-amorphized bulk-crystal Si substrate [see Fig. 3(a) in Ref. 12].

The role that the hydrogen in the amorphous Si layer plays in IBIEC and in the crystallization induced by furnace annealing is discussed in detail elsewhere.[25] According to that article, the rate of epitaxial crystallization is enhanced by the presence of hydrogen in the absence of oxygen. It is shown that the rate of IBIEC for such amorphous Si layer is even higher than that for the implantation-amorphized bulk-crystal Si substrate. The most important factor that determines the rate of IBIEC or the rate of crystallization induced by furnace annealing is the O concentration. But when it is under the threshold value of $2\times10^{19}/\mathrm{cm}^3$, the rates of crystallization are controlled and enhanced by H concentration.

V. SUMMARIES

Layer-by-layer epitaxial crystallization to the surface for LP-CVD amorphous Si layers on (100)-crystal Si substrates is successfully performed by furnace annealing at 600 °C. The relatively high areal density of oxygen at the deposited interface, $\sim1\times10^{15}/\mathrm{cm}^2$, completely prohibits the growth of isolated-epitaxial-columns at the interface or layer-by-layer epitaxial crystallization during furnace annealing. But the diffusion of O atoms can be enhanced by irradiating the layers with a 1-MeV Xe-ion-beam to a dose of $2\times10^{15}/\mathrm{cm}^2$ at 310 °C and this results in layer-by-layer epitaxial crystallization occurring during furnace annealing at 600 °C. With lower-energy ion-beam irradiation, O profiles are also broadened and columnar-epitaxial-growth occurs during furnace annealing at 600–800 °C. This columnar growth is followed by lateral crystallization into the surrounding amorphous region. In all cases that the polycrystallization or the columnar growth occurs by furnace annealing, 1-MeV Xe-ion-beam irradiation induces layer-by-layer epitaxial crystallization at 310 °C.

The diffusion of O atoms at the initial interface is enhanced by high-energy heavy-ion-beam irradiation. This enhancement can be attributed to the inelastic electronic scattering of the incident ion beam under the same elastic nuclear scattering conditions.

The rate of layer-by-layer IBIEC for the sample heated after evacuation is twice as high as that for the sample heated before evacuation. The O content in the former sample is one-third of that in the latter sample.

ACKNOWLEDGMENTS

The author expresses sincere thanks to Dr. T. Makino and Dr. K. Kurihara for their encouragement. The author is indebted to Dr. Y. Kunii and Dr. Y. Takahashi for helpful and fruitful discussions about SPEG of deposited amorphous Si layers. The author also gives thanks to T. Saito for the phosphorus and arsenic implantations and to A. Masamoto for measuring oxygen and hydrogen profiles by high-resolution SIMS. Thanks are also given to Y. Kato and H. Takaoka for taking X-TEM photographs of the LP-CVD samples.

[1] J. Nakata, Phys. Rev. B **43**, 14 643 (1991).
[2] K. A. Jackson, J. Mater. Res. **3**, 1218 (1988).
[3] F. Priolo and E. Rimini, Mater. Sci. Rep. **5**, 319 (1990).
[4] F. Priolo, C. Spinella, and E. Rimini, Phys. Rev. B **41**, 5235 (1990).
[5] J. S. Williams and R. G. Elliman, Phys. Rev. Lett. **51**, 1069 (1983).
[6] J. S. Williams, R. G. Elliman, W. L. Brown, and T. E. Seidel, Phys. Rev. Lett. **55**, 1482 (1985).
[7] M. Fortuna, M.-O. Ruault, H. Bernas, H. GU, and C. Colliex, in *Beam-Solid Interactions*, edited by M. Nastasi, L. R. Harriott, N. Herbots, and R. S. Averback (Materials Research Society, Boston, 1993), p. 547.
[8] J. S. Custer, A. Battaglia, M. Saggio, and F. Priolo, Phys. Rev. Lett. **69**, 780 (1992).
[9] V. Heera, R. Kögler, W. Skorupa, and R. Grotzschel, Nucl. Instrum. Methods Phys. Res. B **80/81**, 538 (1993).
[10] N. Kobayashi, M. Hasegawa, and N. Hayashi, Nucl. Instrum. Methods Phys. Res. B **80/81**, 790 (1993).
[11] V. Heera, T. Henkel, R. Kögler, and W. Skorupa, Phys. Rev. B **52**, 15 776 (1995).
[12] J. Nakata, J. Appl. Phys. **79**, 682 (1996).
[13] V. Heera, J. Appl. Phys. **80**, 4235 (1996).
[14] J. Nakata, J. Appl. Phys. **80**, 4237 (1996).
[15] N. Kobayashi, M. Hasegawa, N. Hayashi, H. Katsumata, Y. Makita, H. Shibata, and S. Uekusa, Nucl. Instrum. Methods Phys. Res. B **100/101**, 498 (1995).
[16] N. Kobayashi, M. Hasegawa, N. Hayashi, H. Katsumata, Y. Makita, H. Shibata, and S. Uekusa, MRS Symposia Proceedings No. 396, Materials Research Society, Boston, 1996 (unpublished), p. 207.
[17] Y. Ohmura, Y. Matsushita, and M. Kashiwagi, Jpn. J. Appl. Phys., Part 2 **21**, L152 (1982).
[18] A. La Ferla, E. Rimini, and G. Ferla, Appl. Phys. Lett. **52**, 712 (1988).
[19] Y. Kunii, M. Tabe, and K. Kajiyama, Jpn. J. Appl. Phys., Part 1 **21**, 1431 (1982).
[20] Y. Kunii and Y. Sakakibara, Jpn. J. Appl. Phys., Part 1 **26**, 1816 (1987).
[21] J. A. Roth and C. L. Anderson, Appl. Phys. Lett. **31**, 689 (1977).
[22] M. von Allmen, S. S. Lau, J. W. Mayer, and W. F. Tseng, Appl. Phys. Lett. **35**, 280 (1979).
[23] L. S. Hung, S. S. Lau, M. von Allmen, J. W. Mayer, B. M. Ullich, J. E. Baker, P. Williams, and W. F. Tseng, Appl. Phys. Lett. **37**, 909 (1980).
[24] J. Nakata, M. Takahashi, and K. Kajiyama, Jpn. J. Appl. Phys. **20**, 2211 (1981).
[25] J. Nakata, J. Appl. Phys. **82**, 5433 (1997).
[26] L. Csepregi, E. F. Kennedy, T. J. Gallagher, J. W. Mayer, and T. W. Sigmon, J. Appl. Phys. **48**, 4234 (1977).
[27] J. Nakata, T. Shibata, Y. Nanishi, and M. Fujimoto, J. Appl. Phys. **76**, 2078 (1994).
[28] J. C. Bourgoin and J. W. Corbett, Rad. Effects **36**, 157 (1978).
[29] T. Yamaguchi and J. Nakata, J. Appl. Phys. **81**, 2219 (1997).
[30] T. Takahashi, Y. Arakawa, N. Nishioka, and T. Ikoma, Appl. Phys. Lett. **60**, 68 (1992).
[31] T. Wada and H. Hada, Phys. Rev. B **30**, 3384 (1984).
[32] T. Wada and Y. Maeda, Appl. Phys. Lett. **52**, 60 (1988).
[33] T. Wada, Appl. Phys. Lett. **52**, 1056 (1988).
[34] H. Akazawa, J. Takahashi, Y. Utsumi, I. Kawashima, and T. Urisu, Appl. Phys. Lett. **60**, 974 (1992).
[35] F. Sato, K. Goto, and J. Chikawa, Jpn. J. Appl. Phys., Part 2 **30**, L205 (1991).